Hindawi Publishing Corporation
International Journal of Antennas and Propagation
Volume 2015, Article ID 873530, 9 pages
http://dx.doi.org/10.1155/2015/873530

Research Article

2D Active Antenna Array Design for FD-MIMO System and Antenna Virtualization Techniques

Ioannis Tzanidis,[1] Yang Li,[1] Gary Xu,[1] Ji-Yun Seol,[2] and JianZhong (Charlie) Zhang[1]

[1] *Wireless Communications Lab, Samsung R&D America, Richardson, TX 75082, USA*
[2] *Advanced Communications Lab., Communications Research Team, DMC R&D Center, Samsung Electronics Corp., 129 Samsung-ro, Yeongtong-gu, Suwon-si, Gyeonggi-do 443-742, Republic of Korea*

Correspondence should be addressed to Ioannis Tzanidis; i.tzanidis@samsung.com

Received 12 February 2015; Revised 28 April 2015; Accepted 13 May 2015

Academic Editor: Xiu Yin Zhang

Full dimension MIMO (FD-MIMO) is one of the key technologies presently studied in the 3GPP for the next generation long-term evolution advanced (LTE-A) systems. By incorporating FD-MIMO into LTE/LTE-A systems, it is expected that system throughput will be drastically improved beyond what is possible in conventional LTE systems. This paper presets details on the 2D active antenna array design for FD-MIMO systems supporting 32 antenna elements. The FD-MIMO system allows for dynamic and adaptive precoding to be performed jointly across all antennas thus achieving more directional transmissions in the azimuth and elevation domains simultaneously, to a larger number of users. Finally, we discuss 2D antenna array port virtualization techniques for creating beams with wide coverage, necessary for broadcasting signals to all users within a sector, such as the CRS (Common Reference Signal).

1. Introduction

Recently, due to the expansion of new mobile smart devices and applications that require considerably larger amount of data compared to traditional voice calls, the wireless communication has experienced a significant increase of wireless data flow on a global scale [1]. Among such techniques are multiple-input multiple-output (MIMO), coordinated multipoint (CoMP) transmission/reception, and carrier aggregation (CA). CoMP relies on coordination between multiple transmission and reception points to enhance user equipment (UE) performance at cell edges but requires a very capable backhaul connection for intersite coordination. Carrier aggregation simultaneously utilizes multiple frequency bands to enhance peak data rate and a network's load balancing capability but requires the use of large frequency resources. Although each of these techniques represents a major step forward in improving system performance, further development of new technologies is required to meet the exponentially growing demand for wireless data traffic. In the meantime, the Third Generation Partnership Project (3GPP) has pushed the standardization efforts on these emerging techniques, including FD-MIMO technology [2].

Full dimension MIMO (FD-MIMO) is one of the key technologies expected to boost the performance of LTE systems. One of the key technologies in FD-MIMO that leads to the impressive improvement on system throughput is to support up to 64 antenna ports placed in a 2D array. As compared to CoMP and CA, FD-MIMO is capable of enhancing system performance without requiring a very capable backhaul system or large frequency resources. Due to the large number of antenna elements it is a big challenge to accommodate high-order multiuser MIMO (MU-MIMO) transmission and reception without complicating the design and implementation of the devices in both base station and user (UE) sides to an impractical level. High-order MU-MIMO refers to the use of a large number of antennas at the base station to transmit or receive spatially multiplexed signals to or from a large number of terminals. Figure 1 depicts an overview of a FD-MIMO system. A 2D antenna array plane, deploying much more antenna elements than the traditional multiple antenna systems in wireless cellular

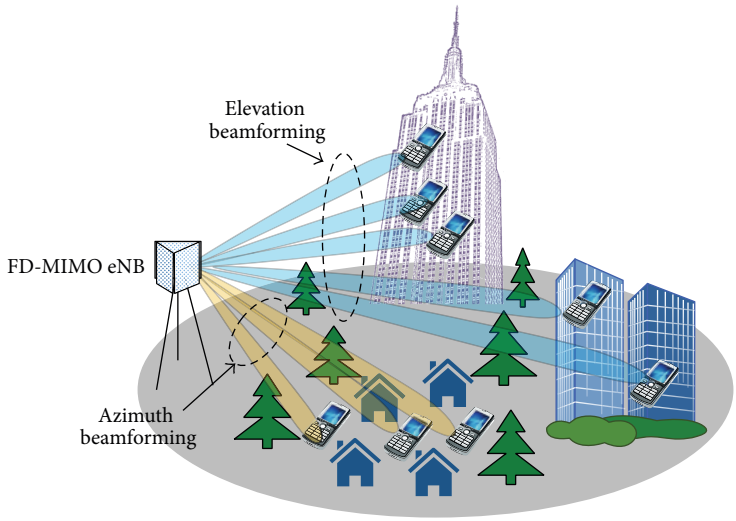

Figure 1: Conceptual diagram of FD-MIMO system realizing high-order MU-MIMO by utilizing 2D antenna array.

communications, is placed on the FD-MIMO base station. The antenna elements allow dynamic and adaptive precoding to be performed jointly across all antennas. As a result of such precoding, the base station achieves more directional transmissions in the azimuth and elevation domain simultaneously to a larger number of UEs.

The need for 3D beamforming demands a 3D Spatial Channel Model (SCM) where each signal path is assigned an angle in both azimuth and elevation domains. A key challenge for 3D SCM is to model the correlation of large scale parameters such as ASD (azimuth spread at departure), ASA (azimuth spread at arrival), ESD (elevation spread at departure), ESA (elevation spread at arrival), shadow fading, Rician K-factor, delay spread, and also the statistical distribution of elevation angles. In 3GPP a study item [2] will finalize the details of 3D SCM.

On the hardware implementation of FD-MIMO, a very important step is the design of a 2D active antenna array [3], that is, the choice of antenna array configuration, the number of horizontal and vertical elements, their polarization type (dual-linear, diagonal, etc.), and the element spacing (uniform, nonuniform, etc.). The key to this decision is a system level simulation, which is performed to analyze various antenna array configurations and compare their throughput with respect to a baseline design. The array configuration with the largest throughput is chosen. This is presented in Section 2. Section 3 presents the actual antenna element design, which entails the antenna element type, the antenna feed, and the antenna performance metrics such as the gain, beamwidth, bandwidth, polarization, and antenna isolation as dictated by the system simulations. The antenna array is then fabricated and measured in the anechoic chamber.

Another very important design step is antenna array port virtualization. 2D large antenna arrays are very suitable for forming narrow beams to multiple users simultaneously, but in a MIMO system there is also need for wide beams that transmit the same signal to all users in a sector at the same time. Forming such wide beams could be resolved by transmitting from a single antenna element (since the element beamwidth is usually equal to the sector beamwidth); however, the transmitted power can be very low, resulting in limited coverage. In that regard it would be desirable to transmit from all 2D antenna array elements simultaneously and to be able to generate a beam with prescribed coverage. In Section 4 we compare various antenna array port virtualization techniques.

2. 2D Antenna Array Architectures

Choosing the most suitable 2D antenna array configuration is the most important step in realizing the gains of FD-MIMO technology. This refers to choosing the number of antennas in the horizontal (H) and vertical (V) dimension of the array, the polarization type (linear, dual-linear, alternating, colocated, etc.), and the element spacing in H and V dimensions. These parameters are impossible to determine without carrying out extensive numerical simulations in a system level. The deployment scenario (Urban Macro, Small Cell, etc.), the channel model, and the UE dropping (indoor, outdoor, vertical distribution, etc.) as well as scheduling algorithms are important simulation parameters that determine a suitable antenna array configuration. Figure 2 shows our simulation assumptions and comparison of four different antenna array configurations. All four configurations assume 32 antennas in an 8H $\times$ 4V configuration on the base station. In this example we study the effect of two different values of element spacing (0.5λ and 2λ) in the vertical dimension of the array (or elevation spacing, El. spacing) while the horizontal spacing (or azimuth spacing, Az. spacing) is fixed at 0.5λ. For each of these two values of antenna spacing we consider two different polarization arrangements, a colocated dual-diagonal polarization (X-pol) antenna element arrangement and an alternating dual-diagonal polarization (Alt.-pol) arrangement as shown in Figure 2 at the bottom. In practice

FD-MIMO: 8H × 4V TX

FD-MIMO antenna configuration	Az. spacing	El. spacing	Az. beamwidth/ Am	El. beamwidth/ SLAv	Antenna gain
Number 1	0.5λ	0.5λ	65°, Am = 30 dB	65°, SLAv = 30 dB	8 dBi
Number 2	0.5λ	2λ	65°, Am = 30 dB	20°, SLAv = 30 dB	12 dBi

Baseline: 4H × 1V TX

eNB antenna configuration (H × V)	4 × 1 (baseline)
Subarray gain	17 dBi
Azimuth beamwidth	70°
Elevation beamwidth	10°
Front-to-back radio	25 dB
Electrical downtilt	12°

Simulation setup:
(i) 3D ITU, UMa
(ii) 57 sectors with $K = 10/15$ UEs per sector
(iii) Center frequency 2 GHz, bandwidth 10 MHz
(iv) UE speed 3 km/h
(v) 20% outdoor, 80% indoor UEs
(vi) UE: 2 Rx (H-V-pol)
(vii) BS: X-pol, down-tilt 12°

(a)

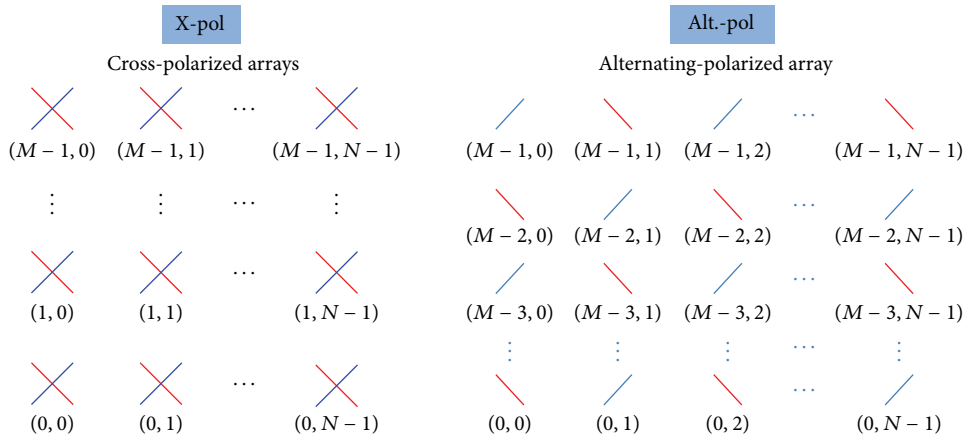

(b)

Figure 2: Comparison of four FD-MIMO antenna array architectures: two different antenna array configurations (0.5λ and 2λ antenna element spacing in elevation) and two different antenna array polarization arrangements (a colocated cross-polarized array is referred to as X-pol, and an alternating-polarized array is referred to as Alt.-pol). Baseline configuration is shown on the top right of (a). Simulations assumptions are also given.

the X-pol antenna would be a dual-linearly polarized antenna element, while the Alt.-pol antenna would be a single linearly polarized antenna element. These antenna array configurations are compared against a baseline LTE eNB antenna array configuration shown in Figure 2 on the right.

The system level simulation results for the above four array architectures is shown in Table 1. The antenna array configuration that yields the largest throughput gains is that of 2λ vertical spacing (El. spacing) and alternating polarization (Alt.-pol). This implementation is presented in the following section. Using our specific antenna parameters in conjunction with a 3D Spatial Channel Model (SCM) we report a promising average cell throughput gain (compared to the base line 4TX design) of approximately 4 times and cell edge throughput gain of 8.2x, (namely, 8.2 times higher throughput) compared to our baseline: a 4TX state-of-the-art 4G LTE system. Simulation results are shown in Table 1.

3. 2D Active Antenna Array Design and Performance

In order to realize the benefit of FD-MIMO, an efficient implementation of a 2D antenna array is a key requirement [4–6]. An actual functioning example of an FD-MIMO array configuration is shown in Figure 3. As dictated by the system level simulations, the array comprises 32 subarrays, which comprise our antenna elements in an 8H × 4V configuration. Each antenna element is actually a subarray configuration (1H × 4V) of four single patch antennas fed by a common feed port. The spacing between two adjacent subarrays is $d_H = 0.5\lambda$ in the horizontal direction and $d_V = 2\lambda$ in the vertical direction (between centers of adjacent subarrays). Each subarray is composed of four patch antenna elements fed with equal magnitude and phase by a single feed port. Thus, the FD-MIMO array has a total of 32 feed ports (corresponding to

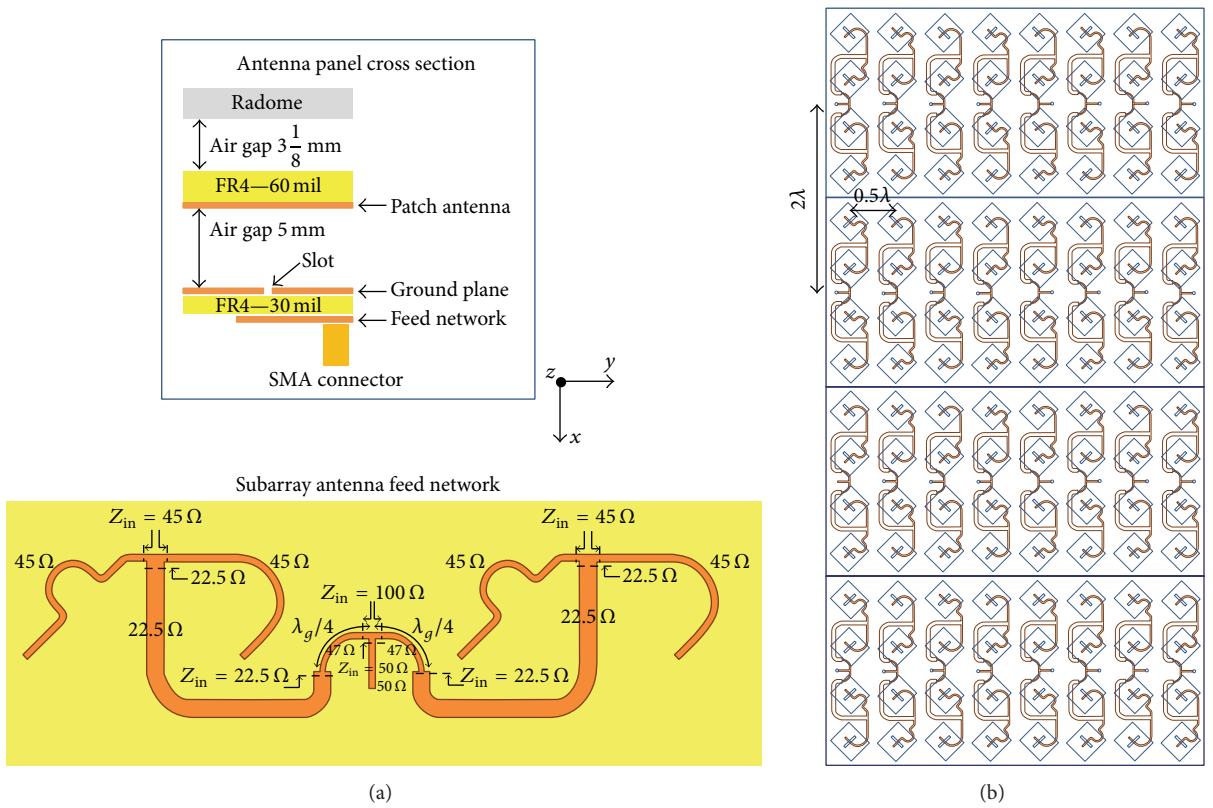

Figure 3: (a) Bottom view of one subarray feed network and detailed PCB stack-up, and (b) top-to-bottom view of FD-MIMO antenna array unit and feed network.

Table 1: System level simulation of antenna array architectures. Throughput gain compared to the baseline design of 4TX antennas.

Antenna array type	Throughput gain (over baseline 4TX)	
	Cell avg.	Cell edge
Config. 1 (0.5λ)		
X-pol	2.4x	4.15x
Alt.-pol	3.3x	5.5x
Config. 2 (2λ)		
X-pol	3.5x	5x
Alt.-pol	**4x***	**8.2x***

*Our implementation.

32 channels) and a form factor of approximately 1 m in height by 50 cm in width.

One of the key features of this FD-MIMO array configuration is that the patch antenna elements are arranged in the $\varphi = \pm 45^{\circ}$ directions which results in linear polarization on the two diagonal planes ($\varphi = \pm 45^{\circ}$ with reference to the coordinate system shown in Figure 3). A close look at the antenna array unit on the right side of the Figure 3 reveals that the patch antenna subarrays are actually alternating orientation (hence, polarization) along the row and column dimension of the array. For instance, in the 4-element subarray at the top left corner of the array unit, patch antennas are rotated such that their polarization plane coincides with the $\varphi = -45^{\circ}$ plane, with respect to the rectangular coordinate system convention shown in Figure 3. Notice that, in the subarray immediately to the right, patch antennas are rotated 90° so that they are polarized on the $\varphi = +45^{\circ}$ plane. This alternating scheme continues along both array dimensions. Due to this configuration, the +45° and −45° polarized subarrays have the same beamwidths in the elevation ($\varphi = 0^{\circ}$) and azimuth ($\varphi = 90^{\circ}$) planes and are affected more alike by the channel characteristics than would a 0° and 90° polarized array version. Notice also that the +45° and −45° subarrays are alternating along both horizontal and vertical directions as dictated by system level simulations. This technique increases the isolation (or decreases coupling) between adjacent subarrays since they are orthogonally polarized.

The patch elements of each subarray are fed through a corporate microstrip line feed network printed on the bottom layer of the feed board. Energy is coupled to the patches through rectangular slot cutouts on the ground plane, on the other side of the feed board. This feeding technique provides better bandwidth, higher isolation between adjacent patch elements, and also more flexibility in adjusting the air-gap between the antenna and feed board (see board stack-up detail in Figure 3) than the conventional probe feeding technique [7]. The air gap between the antenna board and the feed board (ground plane) is tuned so as to maximize the bandwidth and achieve the specified gain and beamwidth as

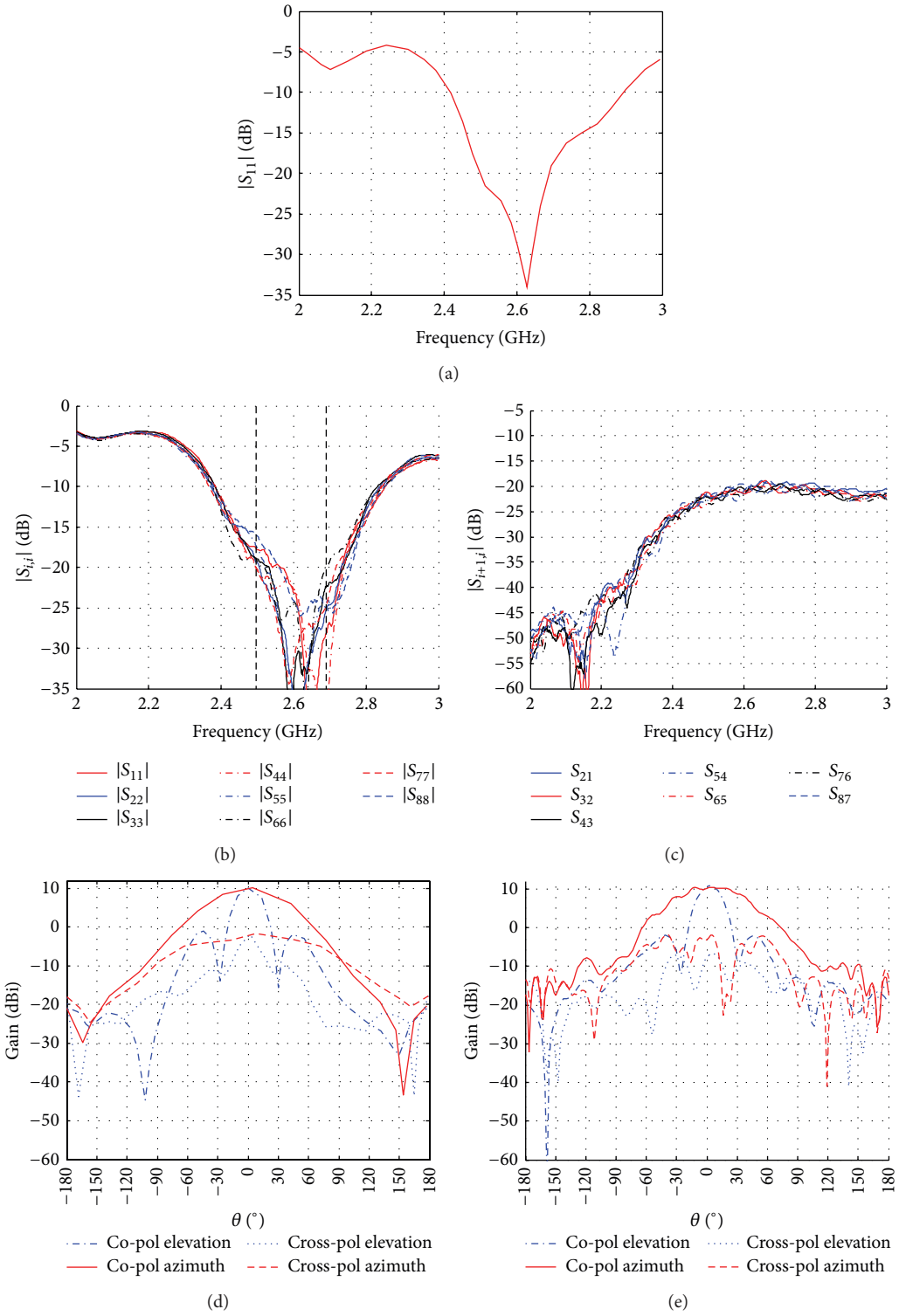

Figure 4: FD-MIMO antenna panel measurements. The panel has 8 alternating polarization subarrays. (a) Simulated reflection coefficient magnitude for a single subarray. (b) Measured reflection coefficient magnitude for 8 subarrays within one FD-MIMO antenna panel. (c) Measured coupling coefficient magnitudes between adjacent subarrays in one panel. (d) Simulated co-pol and cross-pol radiation patterns of one subarray on azimuth ($\varphi = 90^\circ$) and elevation ($\varphi = 0^\circ$) planes at 2.6 GHz. (e) Corresponding measured radiation patterns.

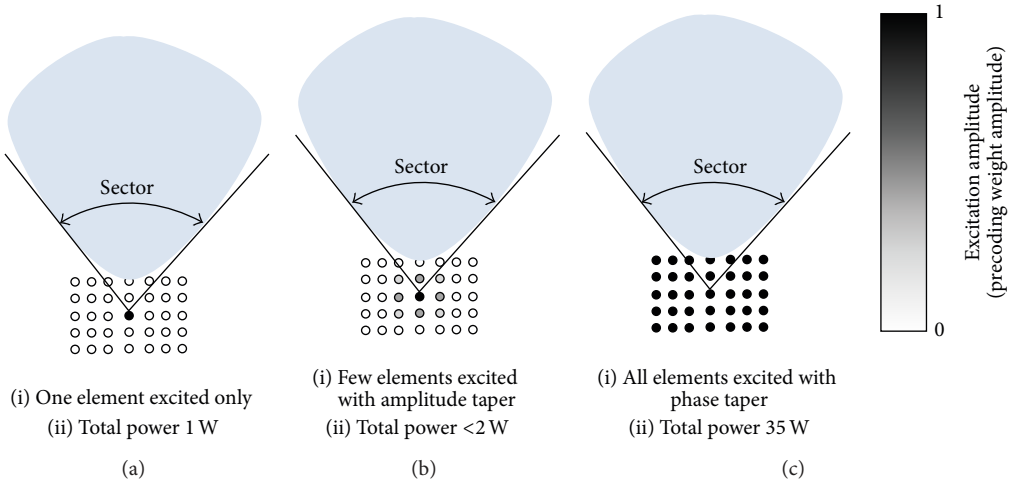

Figure 5: Methods to create wide beam patterns in 2D arrays.

dictated by the system level simulation assumptions shown in Figure 2.

For consistent radiation, it is important that all subarrays be phase matched, that is, the difference of electrical lengths from the feed ports to the patch antennas should not exceed more than $1^\circ \sim 2^\circ$. To ensure phase matching, all subarrays have the same feed network adjusted to fit both $\pm 45^\circ$ rotated patch subarrays by merely mirroring the microstrip sections, as seen in Figure 3 (mirroring sections in our case does not change the electrical length). Further, within each 4-element patch subarray, all microstrip sections were phase matched to better than 1.4°, from the common feed port to each patch antenna.

The antenna is designed to support FD-MIMO in the LTE TDD band #41 (2.496–2.69 GHz) and can achieve a gain of about 10 dBi per subarray with beamwidths of 25° and 65° in the azimuth and elevation domains, respectively. The performance is close to the simulation assumptions of Figure 2. This gain value is the realized gain, which includes the loss in the subarray feed network which was separately measured to be 2.15 dB. Figure 4 shows simulation and measurement results for one panel of the array (8 subarrays) in an anechoic chamber environment. Each subarray has lower than 15 dB return loss (−15 dB reflection coefficient) in the target band while the mutual coupling between adjacent subarrays is below −20 dB. Mutual coupling in patch antenna arrays has been investigated in [8]. Low mutual coupling in conjunction with the high return loss yields very low cross-correlation between antenna ports (less than −35 dB). Simulated and measured copolarized and cross-polarized radiation patterns for one subarray on the azimuth and elevation planes at 2.6 GHz are also shown in Figure 4. The subarray co-pol gain is measured at about 10 dBi at $\theta = 0^\circ$ and the cross-pol gain is measured at about 10 dB below that. The beamwidths on the azimuth and elevation planes are about 65° and 24°, respectively.

4. Antenna Array Port Virtualization

In FD-MIMO systems the use of channel estimation and multiuser precoding algorithms allows the formation of multiple narrow beams allocated to the various users. However, besides the user-specific data transmitted by the narrow beams, FD-MIMO base stations need to broadcast data intended for all users to receive simultaneously, such as control channel and CRS (Common Reference Signal). Such signals cannot be transmitted via a narrow beam but rather via a wide beam with beamwidth that covers the entire sector.

Two methods are generally adopted in practice for generating a wide beam: (1) transmit only from one antenna array element and (2) transmit from multiple elements each with a certain amplitude weighting taper (pattern synthesis) [9]. Both methods have disadvantages. The first method transmits very little power since only one element (out of typically a few decades of elements) is excited. Thus the range is limited and gain control (AGC) is needed on the user side. The second method suffers from a similar problem, since the method synthesizes a given beam pattern resulting in amplitude taper that heavily excites a few antenna elements at the center of the array while the majority of the elements are excited with very little power.

To generate wide beam with all antenna elements excited at full power is not a trivial task, because, in general, a fully excited antenna array generates a narrow beam pattern. Thus, in order to generate a wide beam with certain beamwidths in azimuth and elevation and all antenna elements excited at full power (amplitude equals to 1) a certain phase taper has to be applied. That phase taper has to be somewhat robust, to account for possible phase errors in the phase calibration process.

Figure 5 summarizes the two commonly used methods to generate a 2D wide beam that covers a specific sector angle. Although the sector is shown in 1D (azimuth cut), the reader should visualize a similar sector, yet maybe narrower,

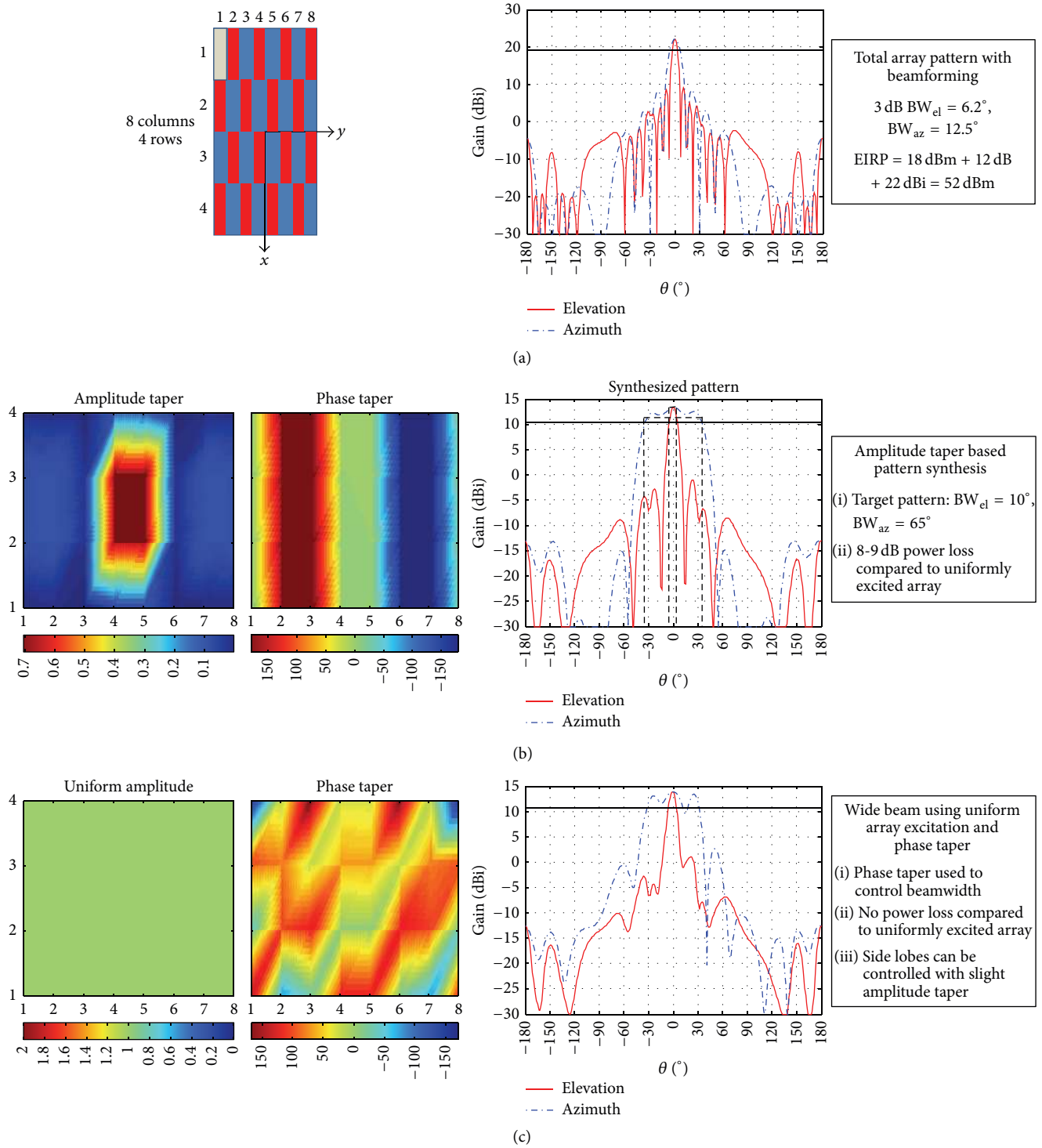

FIGURE 6: (a) Our implementation of a 2D FD-MIMO antenna array with the beamforming gain pattern. (b) A classic method to synthesize a wide beam pattern with specific beam widths in elevation and azimuth, using an aggressive amplitude taper, where the majority of antenna array elements are almost unexcited. (c) Method to generate a wide beam pattern using a phase taper and uniform amplitude taper.

in the second dimension (elevation). As seen in Figure 5 left, a wide beam can be generated by just exciting only one array element. If we assume that the array elements can transmit a maximum power of 1 W, then the first method of exciting only one element (represented by black color) results in only 1 W of power being transmitted and hence in limited coverage and range. The second method (Figure 5 middle), employs pattern synthesis with amplitude taper to synthesize a wide beam. Again, although only one dimension is shown in Figure 1, the reader should visualize

a 2D pattern with azimuth and elevation beamwidths that cover a specific sector. The second method results in slightly higher transmitted power, since only the center element is fully excited (represented by black color), while a few elements to its left and right are only slightly excited (very low amplitude represented by grey color). Still, the majority of array elements are not excited (white color) resulting in low transmitted power and thus limited range.

The third method, illustrated in Figure 5 on the right, shows a technique where all array elements are excited fully with equal amplitudes but different phases. As a result, a desired 2D beam pattern can be generated with the total transmitted power being equal to the maximum available transmitted power of the PA of each antenna element. Thus we can expect the range to be maximized and the requirements on the dynamic range of the AGC to be relaxed.

As an example we apply these techniques to our antenna array shown in Figure 3. Figure 6(a) shows the gain beam pattern on the elevation and azimuth planes when all 32 antenna array elements are excited with the same phase. As seen, the resulting 3 dB beamwidth is about 6.2° in elevation domain and 12.5° in the azimuth domain. If the transmit power per antenna element is assumed to be 18 dBm, then the EIRP will be 18 dBm + 12 dB (PA gain) + 22 dBi (array gain per polarization) = 52 dBm (per polarization).

In Figure 6(b) the amplitude taper method (Fourier Transform Method) is adopted to synthesize a wide beam with 10° beamwidth in elevation and 65° beamwidth in azimuth. As mentioned earlier, the amplitude taper technique leaves the majority of antenna elements not excited (see amplitude taper in Figure 6(b)), resulting in a heavy power loss of the order of 8 dB, as compared to the fully excited array. Thus the PA gain in that case will only be 12 dB − 8 dB = 4 dB and thus the EIRP will drop to 18 dBm + 4 dB (PA gain) + 12 dBi (array gain per polarization) = 34 dBm. This can result in very limited range.

In Figure 6(c) we demonstrate the phase taper technique. This technique excites all antenna elements with full power, thus maintaining full PA gain while it shapes the pattern to the specified beamwidths by phase taper. The resulting beam pattern using the phase taper method is shown in Figure 6(c). The result of the phase taper is an EIRP of about 42 dBm.

One concern when dealing with phase weights is the sensitivity to phase errors. Phase errors occur from many sources such as temperature variation of active components, part-by-part variation in passive components, and nonuniform dielectric substrates. To account for these phase inconsistencies advanced calibration methods are employed which adjust the phase of each active chain at the baseband level such that all signals arrive at the antenna ports with the prescribed phase weights. Antenna calibrations are regular intervals during system operation. Despite calibration, FD-MIMO arrays with large number of active chains can never be perfectly phase calibrated. For small array (<8 antennas), calibration aligns channels to within a few degrees of error (about ±5°). If the phase error between channels is more than 10°, the calibration circuit might not be performing adequately. For arrays with many active chains calibration errors can be higher because of error propagation in calibration methods [10]. Thus, a phase taper method for generating wide beam patterns has to be able to maintain its robustness despite small phase uncertainties.

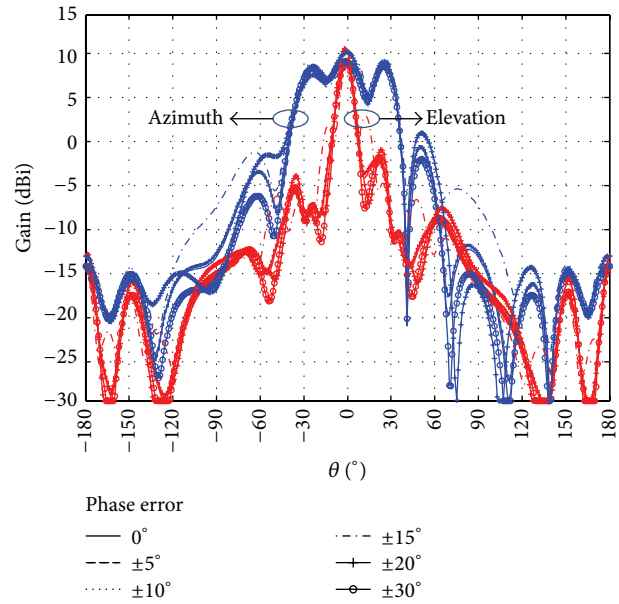

Figure 7: Robustness of phase taper method to phase errors.

Figure 7 shows the performance of the phase taper technique in presence of random phase errors of a maximum of ±5° up to ±30°. We would like to note that during our phase error analysis a phase error, for example, of ±15° meant that the phase of some randomly selected elements was allowed to vary up to that amount. Still, most antenna elements were randomly assigned a phase error of less than ±15°. As seen in Figure 7, the phase taper method is somewhat robust to phase errors. Phase errors primarily affect the gain ripple within the main lobe and also side lobe levels. We noticed that beyond ±30° of maximum phase error beamwidth was affected more heavily. Because all antenna array elements are excited with uniform amplitude (see Figure 6(c)), random errors in the phase taper method can be balanced out in wide beamwidth cases and for arrays with many elements, and this is the reason why the phase taper method exhibits robustness to phase errors.

5. Conclusions

In this paper, we presented the design and performance of a FD-MIMO 2D active antenna array system. We carried out system level simulations to compare various antenna array configurations and understand their impact on the system performance (throughput gain). We found that 2λ antenna spacing and alternating polarization scheme yields the highest throughput gains with a practically realizable form factor. Further, we designed and measured the antenna array that meets the assumptions of the system level simulation. Finally, we compared two methods for generating wide beam pattern in large 2D FD-MIMO arrays. Such wide beams are required for signals that are intended to be transmitted not separately

to each user but to a whole sector of specific azimuth and elevation dimensions. We found that the amplitude taper method can result in low transmitted power and thus in low range, whereas the phase taper method can maintain full transmit power and is robust to phase errors of up to ±30°.

Conflict of Interests

The authors declare that there is no conflict of interests regarding the publication of this paper.

References

[1] Cisco, *Cisco Visual Networking Index: Global Mobile Data Traffic Forecast Update, 2012–2017*, Cisco, 2013.

[2] 3GPP TSG RAN Plenary #58, R1-122034, Study on 3D-channel model for Elevation Beamforming and FD-MIMO studies for LTE, Barcelona, Spain, 2012.

[3] B. L. Ng, Y. Kim, J. Lee et al., "Fulfilling the promise of massive MIMO with 2D active antenna array," in *Proceedings of the IEEE Globecom Workshops (GC Wkshps '12)*, pp. 691–696, December 2012.

[4] Y.-H. Nam, B. Ng, K. Sayana et al., "Full-dimension MIMO (FD-MIMO) for next generation cellular technology," *IEEE Communications Magazine*, vol. 51, no. 6, pp. 172–179, 2013.

[5] Y. Kim, H. Ji, J. Lee et al., "Full dimension mimo (FD-MIMO): the next evolution of MIMO in LTE systems," *IEEE Wireless Communications*, vol. 21, no. 2, pp. 26–33, 2014.

[6] S. Akoum and J. Acharya, "Full-dimensional MIMO for future cellular networks," in *Proceedings of the IEEE Radio and Wireless Symposium (RWS '14)*, pp. 1–3, Newport Beach, Calif, USA, January 2014.

[7] M. Civerolo and D. Arakaki, "Aperture coupled patch antenna design methods," in *Proceedings of the IEEE International Symposium on Antennas and Propagation (APSURSI '11)*, pp. 876–879, July 2011.

[8] D. R. Jackson, W. F. Richards, and A. Ali-Khan, "Series expansions for the mutual coupling in microstrip patch arrays," *IEEE Transactions on Antennas and Propagation*, vol. 37, no. 3, pp. 269–274, 1989.

[9] C. A. Balanis, *Antenna Theory: Analysis and Design*, Wiley Interscience, 3rd edition, 2005.

[10] J. McCormack, T. Cooper, and R. Farrell, "Tower-top antenna array calibration scheme for next generation networks," *EURASIP Journal on Wireless Communications and Networking*, vol. 2007, Article ID 41941, 2007.